Hindawi Publishing Corporation
Journal of Nanomaterials
Volume 2013, Article ID 612153, 8 pages
http://dx.doi.org/10.1155/2013/612153

Hindawi

Research Article

Electronic Structures and Optical Properties of Phenyl C_{71} Butyric Acid Methyl Esters

Cai-Rong Zhang,[1,2] Li-Heng Han,[1] Jian-Wu Zhe,[3] Neng-Zhi Jin,[3] Yu-Lin Shen,[3] Li-Hua Yuan,[1] You-Zhi Wu,[2] and Zi-Jiang Liu[4]

[1] *Department of Applied Physics, Lanzhou University of Technology, Lanzhou, Gansu 730050, China*
[2] *State Key Laboratory of Gansu Advanced Non-Ferrous Metal Materials, Lanzhou University of Technology, Lanzhou, Gansu 730050, China*
[3] *Gansu Computing Center, Lanzhou, Gansu 730030, China*
[4] *Department of Physics, Lanzhou City University, Lanzhou 730070, China*

Correspondence should be addressed to Cai-Rong Zhang; zhcrxy@lut.cn

Received 20 September 2013; Accepted 11 November 2013

Academic Editor: Jinlong Jiang

Phenyl C_{71} butyric acid methyl ester ($PC_{71}BM$) has been adopted as electron acceptor materials in bulk heterojunction solar cells with relatively higher power conversion efficiency. The understanding of the mechanism and performance for the devices based upon $PC_{71}BM$ requires the information of conformations, electronic structures, optical properties, and so forth. Here, the geometries, IR and Raman, electronic structures, polarizabilities, and hyperpolarizabilities of $PC_{71}BM$ isomers are studied by using density functional theory (DFT); the absorption and excitation properties are investigated via time-dependent DFT with B3LYP, PBE0, and CAM-B3LYP functionals. The calculated results show that [6,6]$PC_{71}BM$ is more stable than [5,6]$PC_{71}BM$ due to the lower total energy. The vibrational modes of the isomers at IR and Raman peaks are quite similar. As to absorption properties, CAM-B3LYP functional is the suitable functional for describing the excitations of $PC_{71}BM$ because the calculated results with CAM-B3LYP functional agree well with that of the experiment. The analysis of transition configurations and molecular orbitals demonstrated that the transitions at the absorption maxima in UV/Vis region are localized π-π^* transitions in fullerenes cages. Furthermore, the larger isotropic polarizability of $PC_{71}BM$ indicates that the response of $PC_{71}BM$ to applied external electric field is stronger than that of $PC_{61}BM$, and therefore resulting into better nonlinear optical properties.

1. Introduction

The electronic devices based upon organic materials, such as organic radiofrequency identification, light emitting diode, memory devices, and solar cells, have attracted considerable attention in the past decade due to their potential to be lower-cost, light-weight, flexible, and large-area equipment. These devices usually contain heterojunction formed by electronic donor and acceptor materials. The properties of materials in these devices, including chemical structures [1], electronic structures [2], excited states [3], charge transfer, and charge transport [4], are of particular importance for their overall performance. To provide a better understanding toward the higher performance of device, it is necessary to investigate the electronic structures of the materials, as well as the energy level alignment at the heterojunction interface [5]. The discovery of ultrafast photoinduced charge/energy transfer from a conjugated polymer to fullerene molecules and introducing bulk heterojunction (BHJ) stimulated the rapid development of organic photovoltaic (OPV) technology [4, 6–11]. Also, some fullerene hybrids show good nonlinear optical properties [12].

Among the fullerene derivatives in OPV, [6,6]-phenyl-C_{61} butyric acid methyl ester ($PC_{61}BM$) as the soluble electron acceptor was widely used to fabricate efficient BHJ organic polymer solar cells (PSCs) [13]. For instance, Svensson et al. reported the PSC with open circuit voltage (V_{oc}) 1 V based on alternating copolymer PFDTBT blended with

$PC_{61}BM$ [14]. Inganäs et al. performed a systematic study of PSCs and found the efficiency about 2-3% using four different fluorene copolymers through changing the length of the alkyl side chains and chemical structures [15]. A series of highly soluble fullerene derivatives with varying acceptor strengths was applied in PSCs, and the V_{oc} of the corresponding devices was found to correlate directly with the acceptor strength of the fullerenes [16]. Unfortunately, $PC_{61}BM$ has very low absorption coefficients in UV/Vis region [17], which limits the light harvesting efficiency.

Phenyl C_{71} butyric acid methyl ester ($PC_{71}BM$), a higher fullerene analogue of $PC_{61}BM$, displays improved light absorption in the visible region of spectrum [17, 18]. $PC_{71}BM$ was adopted as electron acceptor in BHJ solar cells with relatively higher power conversion efficiency (PCE) [19–25]. The substitution of $PC_{61}BM$ with $PC_{71}BM$ under the same standard test conditions in PSC increased current densities about 50% [26], as well as approached to 3.0% of PCE [17]. Recently, more than 10% PCE has been reported by PSCs of PCDTBT:$PC_{71}BM$ system [27].

$PC_{71}BM$ has similar geometry to $PC_{61}BM$, and the fullerene cage of $PC_{71}BM$ contains ten C atoms more than that of $PC_{61}BM$, but the performances of them in PSCs are quite different. The better understanding of the mechanism and performance for the devices based upon $PC_{71}BM$ requires the information of conformations, electronic structures, optical properties, and so forth. In this work, taking into account two kinds of possible isomers of phenyl C_{71} butyric acid methyl esters, the geometries, electronic structures, vibrational properties, polarizabilities, and hyperpolarizabilities are calculated using density functional theory (DFT), and the absorption properties which relate to the character of excited states are addressed with time-dependent DFT (TDDFT) [28–34]; the comparative analyses for the isomers are also reported.

2. Computational Methods

The computations of the geometries and vibrational properties have been performed with Becke's three parameters gradient-corrected exchange potential and the Lee-Yang-Parr gradient-corrected correlation potential (B3LYP) [35–38], since the comparison with the MP2 geometries of several organic molecules confirmed the accuracy of B3LYP for the geometry optimizations [39]. In order to get the reliable calculations of absorption spectra and excited states, the hybrid functionals B3LYP and PBE0 [40–42], as well as long-range-corrected hybrid functional Coulomb attenuation method CAM-B3LYP [43], are adopted in TDDFT calculations. The comparison of absorption spectra between experiment and calculations demonstrates the better performance of CAM-B3LYP functional in describing the excited state properties of $PC_{71}BM$. Thus, the electronic structures, polarizabilities, and hyperpolarizabilities are also analyzed using CAM-B3LYP functional. The nonequilibrium version of the polarizable continuum model (PCM) [44] is employed to take account of the solvent effects of toluene solution. The polarized split-valence 6-31G(d,p) basis sets are sufficient for calculating the excitation of organic molecules [45], and introducing additional diffuse functions in basis sets generates negligible effects on the electron density and hence on the accuracy of DFT and TDDFT results [39]. All calculations were performed with 6-31G(d,p) basis sets without any symmetry constraints using the Gaussian 09 package [46].

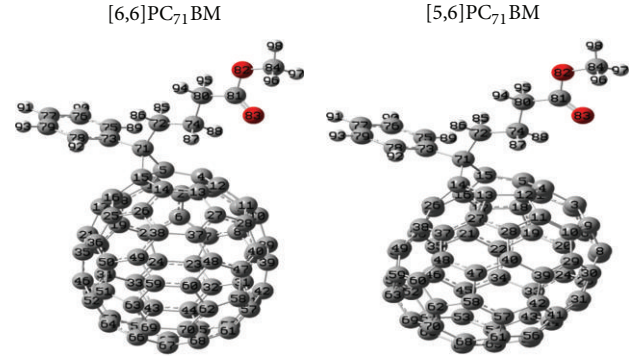

Figure 1: The optimized geometrical structures of [6,6]$PC_{71}BM$ and [5,6]$PC_{71}BM$ in gas phase (gray circles: C red circles: O; light gray circles: H).

3. Results and Discussion

3.1. Geometrical Structures. C_{70} fullerene is composed of 12 five-C rings and 25 six-C rings with D_{5h} symmetry. However, when the C atom in the side chain of butyric acid methyl ester connects to C_{70} cage, two possible isomers can be formed since the C atom can connect to not only the most "polar" carbon-carbon double bonds in C_{70} (the adjacent edge of six-C rings), but also the carbon-carbon single bond in C_{70} (the adjacent edge between five-C rings and six-C rings), and these two structures were denoted as [6,6]$PC_{71}BM$ and [5,6]$PC_{71}BM$, respectively. The isomerization is similar to other fullerene derivatives [47].

The optimized geometries of [6,6]$PC_{71}BM$ and [5,6]$PC_{71}BM$ at the B3LYP/6-31G(d,p) level in gas phase are shown in Figure 1. The calculated total energy of [6,6]$PC_{71}BM$ is about 0.54 eV lower than that of [5,6]$PC_{71}BM$. The NMR spectrum confirmed the stability of [6,6]$PC_{71}BM$ isomer [17]. The selected bond lengths, bond angles, and dihedral angles are listed in Tables s1 and s2 in Supplementary Material available online at http://dx.doi.org/10.1155/2013/612153. The calculated average bond lengths of single and double bonds in fullerene cage of $PC_{71}BM$ isomers are about 0.145 and 0.141 nm, respectively, which are very close to the corresponding values (0.145 and 0.140 nm) of C_{70} fullerene obtained from the same level of theoretical calculation. The bond character of C5–C15 was changed from double bond (0.140 nm) in pure C_{70} fullerene to single bond (0.163 nm) in [6,6]$PC_{71}BM$ due to forming a carbon trigon (C5–C15–C71) through the changes of orbital hybridization, and the change of C5–C15 bond length is similar to the cases of C_{60}-TPA [48] and N-methyl-3,4-fulleropyrrolidine [49], while, in [5,6]$PC_{71}BM$, the atomic distance between C14 and C15 is about 0.213 nm, which far exceeds the typical C–C

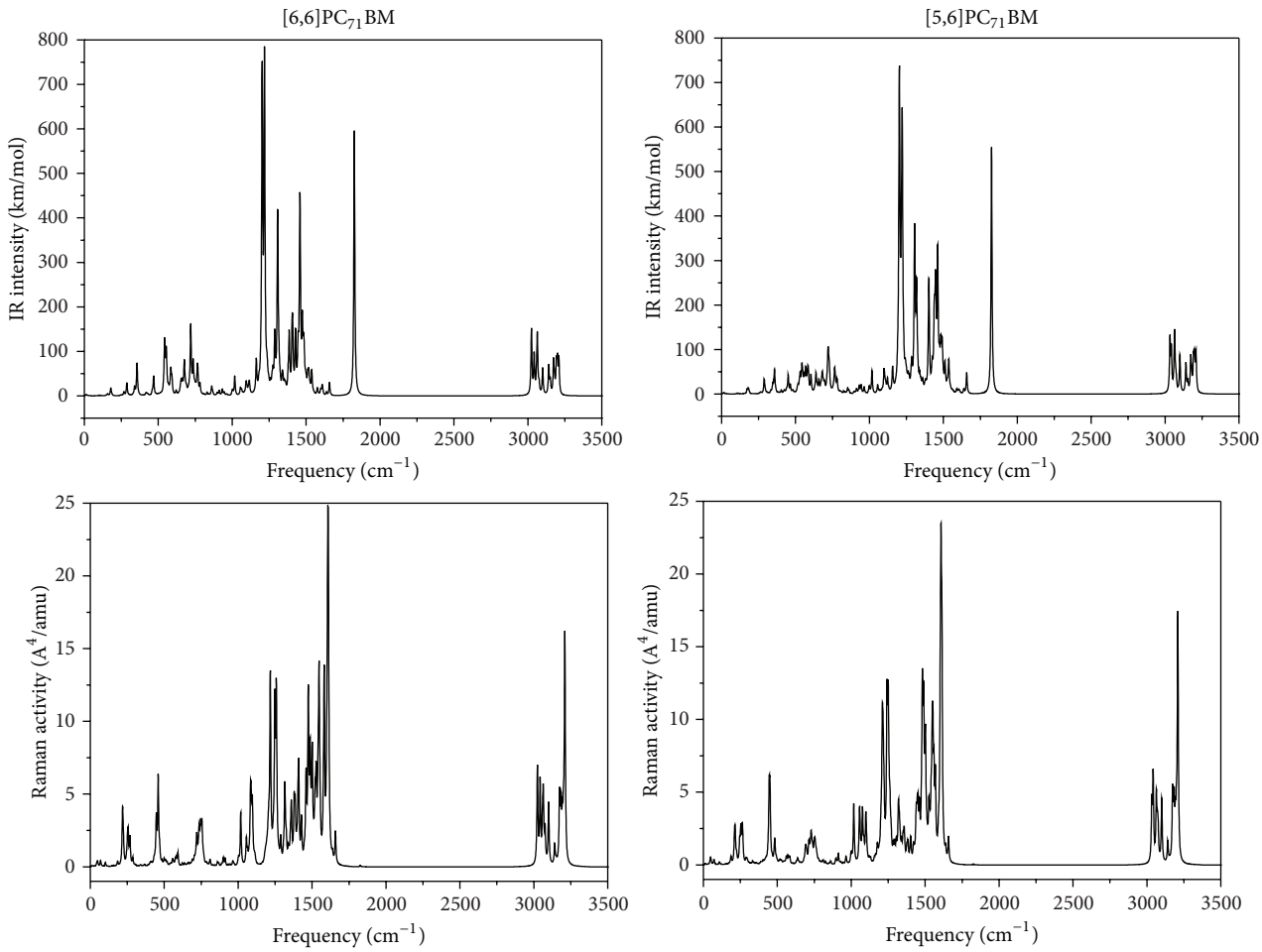

Figure 2: The IR and Raman spectra of $[6,6]PC_{71}BM$ and $[5,6]PC_{71}BM$. The top panel is IR spectra, while the bottom panel is Raman spectra.

single bond length (0.154 nm). Therefore, the single bond of C14–C15 is broken in the isomer. This is the main difference between the two isomers and it may affect electronic and optical properties. The other corresponding geometrical parameters of these isomers are very similar because of the localized character of chemical bonds.

3.2. IR and Raman. In order to investigate the IR and Raman properties of $PC_{71}BM$, the vibrational analyses are performed based upon the optimized structures of isomers. The IR and Raman spectra of $[6,6]PC_{71}BM$ and $[5,6]PC_{71}BM$ are shown in Figure 2. The calculated vibrational data indicates that there are no imaginary frequencies. This means that the optimized isomer structures are the minima of potential energy surface indeed.

The vibrational frequency ranges of $[6,6]PC_{71}BM$ and $[5,6]PC_{71}BM$ are 10~3210 cm^{-1} and 13~3209 cm^{-1}, respectively. For $[6,6]PC_{71}BM$, the strongest IR peaks at about 1219 and 1203 cm^{-1} correspond to the C–H bond-bending vibrational modes in butyric acid methyl ester group, while the IR peak at about 1826 cm^{-1} comes from stretch mode of C–O bond in carbonyl group. As to $[5,6]PC_{71}BM$, the vibrational modes of the strongest peaks at about 1222 and 1826 cm^{-1} are very similar to those of $[6,6]PC_{71}BM$, whereas to Raman, for $[6,6]PC_{71}BM$, the peak at about 1609 cm^{-1} comes from the stretching mode of C–C bonds in the fullerene cage, and the peak at about 3210 cm^{-1} relates to the stretching mode of C–H bonds in phenyl group. Again, the vibrational modes of peaks at about 1608 and 3209 cm^{-1} for $[5,6]PC_{71}BM$ are very similar to those of $[6,6]PC_{71}BM$. Furthermore, the strengths of IR and Raman at the strongest peaks of $[6,6]PC_{71}BM$ are slightly larger than those of $[5,6]PC_{71}BM$ due to its larger dipole moment. The vibrational modes at the IR and Raman peaks of $PC_{71}BM$ are very similar to those of $PC_{61}BM$ [50] due to the same moiety and the similarity of fullerene cages.

3.3. Absorption Spectra and Electronic Structures. The UV/Vis absorption of $PC_{71}BM$ was measured in toluene solution, and the absorption peaks locate at about 462 and 372 nm, respectively [17]. Also, the experiment demonstrated that the absorption coefficient of $PC_{71}BM$ is significantly higher than that of $PC_{61}BM$ in the visible region [17]. The better absorption properties of $PC_{71}BM$ are favorable for improving light harvesting efficiency in OPV. In order to select a suitable functional for the excitations of $PC_{71}BM$, the B3LYP, PBE0, and CAM-B3LYP functionals are adopted in computing

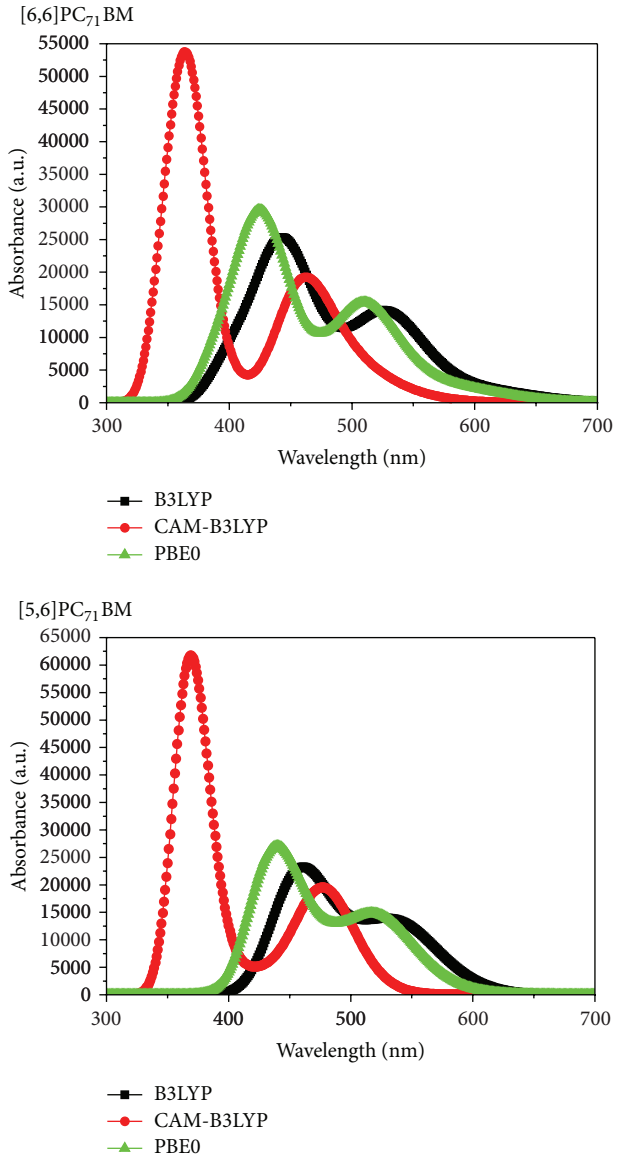

Figure 3: The simulated absorption spectra for $[6,6]PC_{71}BM$ and $[5,6]PC_{71}BM$ based upon TD-DFT results calculated with different functionals. The 0.15 eV of half-width at half-maximum was applied for simulating absorption spectra.

MOs	$[6,6]PC_{71}BM$	$[5,6]PC_{71}BM$
HOMO-3		
HOMO-2		
HOMO-1		
HOMO		
LUMO		
LUMO + 1		
LUMO + 2		
LUMO + 3		

Figure 4: Isodensity plots (isodensity contour = 0.02 a.u.) of the frontier molecular orbitals of $[6,6]PC_{71}BM$ and $[5,6]PC_{71}BM$ with CAM-B3LYP functional.

the absorption spectra of the isomers in toluene solution. The simulated absorption spectra for the two isomers of $PC_{71}BM$ are presented in Figure 3. Apparently, the excitation energies calculated with CAM-B3LYP are larger than the corresponding values calculated with PBE0 and B3LYP functionals due to the different methods for dealing with exchange and correlation energies. Comparing with the experimental results, we found that the CAM-B3LYP functional results agree well with the experimental data.

The excitation properties for the first excited state S_1 and the excited states at absorption peaks in UV-Vis region for $[6,6]PC_{71}BM$ and $[5,6]PC_{71}BM$ in toluene are listed in Table 1, which includes the excitation energies (eV), wavelength (nm), oscillator strengths (f) and the transition configurations with coefficients larger than 10%. The results indicate that the excitation energies at the absorption maxima for the isomers are very close, and the excited states include several transition configurations. To understand the transition character, the molecular orbitals involved transitions in Table 1 are presented in Figure 4. The HOMOs are π orbitals between C–C bonds in fullerene cage, while the LUMOs are π^* orbitals in fullerene. Thus, the transitions in Table 1 are localized π-π^* transitions in fullerenes cages. This is different from that of $PC_{61}BM$, which has several intramolecular charge transfer transitions [50].

The exciton binding energy (EBE), an important quantity for the efficiency of excitonic solar cells, determines the charge separation in solar cells [51]. The EBE can be calculated as the difference between the electronic and optical band gap energies [52]. The electronic band gap is calculated as the energy difference between the HOMO and LUMO levels, while the first excitation energy is adopted as the optical gap [51, 53]. The molecular orbital energy levels and HOMO-LUMO gaps of $PC_{71}BM$ isomers are shown in Figure 5. The HOMO-LUMO gap of $[6,6]PC_{71}BM$ is about 4.34 eV, which is about 0.09 eV smaller than that of $[5,6]PC_{71}BM$. The calculated EBE for $[6,6]PC_{71}BM$ and $[5,6]PC_{71}BM$ are 2.08

Table 1: The excitation energies (eV), wavelength (nm), oscillator strengths (f), and the transition configurations with coefficients larger than 10% for the first excited state S_1 and the excited states at absorption peaks in UV/Vis region for [6,6]PC_{71}BM and [5,6]PC_{71}BM in toluene.

	States	Transition configurations	E (nm/eV)	f
		[6,6]PC_{71}BM		
CAM-B3LYP	S_1	H → L (56%); H → L + 1 (19%); H − 2 → L + 1 (13%)	548/2.26	0.0077
	S_7	H − 2 → L + 1 (56%); H → L + 1 (10%)	456/2.72	0.0770
	S_{22}	H → L + 3 (27%); H − 3 → L + 1 (17%); H − 2 → L + 3 (14%); H − 7 → L + 2 (12%); H − 3 → L (10%)	372/3.33	0.2047
B3LYP	S_1	H → L + 1 (73%); H → L (26%)	621/2.00	0.0020
	S_8	H − 2 → L + 1 (69%)	530/2.34	0.0635
	S_{25}	H − 5 → L + 2 (32%); H − 8 → L (25%); H → L + 3 (16%); H − 3 → L + 1 (10%)	444/2.79	0.0690
PBE0	S_1	H → L + 1 (89%)	597/2.08	0.0003
	S_8	H − 2 → L + 1 (69%)	512/2.43	0.0660
	S_{25}	H − 5 → L + 2 (24%); H − 7 → L + 2 (12%); H − 4 → L + 2 (11%)	425/2.92	0.0817
		[5,6]PC_{71}BM		
CAM-B3LYP	S_1	H → L + 2 (28%); H − 1 → L (22%); H − 2 → L + 1 (15%); H − 1 → L + 2 (12%); H → L (11%)	535/2.32	0.0003
	S_5	H → L (29%); H − 1 → L (25%); H − 2 → L (18%)	478/2.60	0.0864
	S_{29}	H − 3 → L + 2 (26%); H → L + 3 (23%); H − 1 → L + 3 (19%)	365/3.39	0.1991
B3LYP	S_1	H → L (87%)	608/2.04	0.0002
	S_8	H → L + 2 (39%); H − 2 → L (19%); H − 4 → L (13%)	544/2.28	0.0709
	S_{26}	H − 7 → L + 1 (29%); H − 6 → L (22%); H − 7 → L + 2 (14%)	458/2.71	0.0738
PBE0	S_1	H → L (81%)	586/2.12	0.0003
	S_9	H − 1 → L + 2 (44%); H − 2 → L + 1 (23%); H − 4 → L + 1 (10%)	526/2.36	0.0537
	S_{26}	H − 6 → L (26%); H − 7 → L + 1 (25%); H − 7 → L + 2 (11%)	438/2.83	0.0828

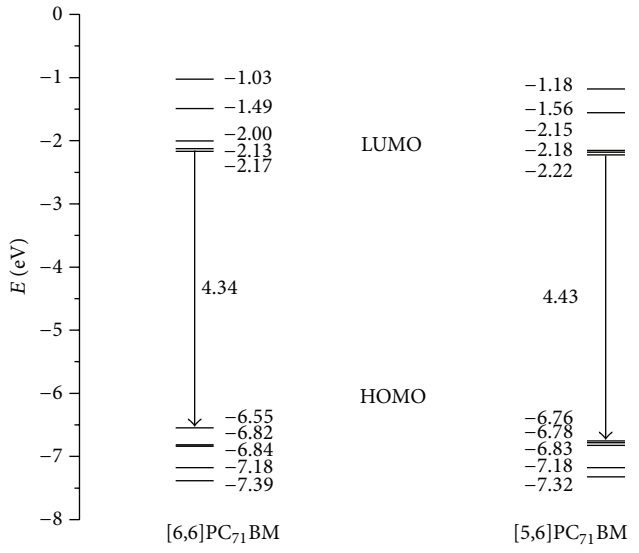

Figure 5: The calculated frontier molecular orbital energies and HOMO-LUMO gaps (in eV) at the CAM-B3LYP/6-31G(d,p) level in toluene solvent.

and 2.11 eV, respectively. The smaller EBE of [6,6]PC_{71}BM is favorable for exciton dissociation in heterojunction.

3.4. Polarizabilities and Hyperpolarizabilities. Polarizabilities and hyperpolarizabilities characterize the response of a system in an applied electric field in some extent [54], such as the strength of molecular interactions, the cross sections of scattering, collision processes, and the nonlinear optical properties of the system [55, 56]. The definition for the isotropic polarizability is

$$\alpha = \frac{1}{3}\left(\alpha_{XX} + \alpha_{YY} + \alpha_{ZZ}\right), \tag{1}$$

the polarizability anisotropy invariant is

$$\Delta\alpha = \left[\frac{\left(\alpha_{XX} - \alpha_{YY}\right)^2 + \left(\alpha_{YY} - \alpha_{ZZ}\right)^2 + \left(\alpha_{ZZ} - \alpha_{XX}\right)^2}{2}\right]^{1/2}, \tag{2}$$

and the average hyperpolarizability is

$$\beta_{\parallel} = \frac{1}{5}\sum_{i}\left(\beta_{iiZ} + \beta_{iZi} + \beta_{Zii}\right), \tag{3}$$

where α_{XX}, α_{YY}, and α_{ZZ} are tensor components of polarizability; β_{iiZ}, β_{iZi}, and β_{Zii} (i from X to Z) are tensor components of hyperpolarizability. For [6, 6]PC_{71}BM, the calculated α_{XX}, α_{YY}, and α_{ZZ} are 818.5, 699.3, and 638.9 a.u., respectively, and the computed β_{XXZ}, β_{YYZ}, and β_{ZZZ} are 67.0, −28.6, and −98.8 a.u., respectively. For [5,6]PC_{71}BM, the corresponding tensor components are 817.1, 711.7, and 614.4 a.u., respectively, and the calculated β_{XXZ}, β_{YYZ}, and β_{ZZZ} are −26.7, −2.4, and −108.4 a.u., respectively. In addition to the individual tensor components of the polarizabilities and the first hyperpolarizabilities, the calculated isotropic polarizability, polarizability anisotropy invariant, and average hyperpolarizability for [6,6]PC_{71}BM are α = 718.9 a.u., $\Delta\alpha$ = 158.3 a.u., and $\beta_{\parallel}$ = −36.2 a.u., respectively, and

the corresponding values for [5,6]PC_{71}BM are 723.4, 153.2, and −82.5 a.u., respectively. The values are larger than that of PC_{61}BM (α = 577.7 a.u., $\Delta\alpha$ = 96.9 a.u., and $\beta_{\parallel}$ = −22.8 a.u. (B3LYP/3-21G*)) [50] due to the C_{70} fullerene cage. This means that PC_{71}BM has stronger response of external field and better nonlinear optical properties than that of PC_{61}BM.

4. Conclusions

In this work, the geometries, IR and Raman, electronic structures, polarizabilities, and hyperpolarizabilities of PC_{71}BM isomers are studied by using DFT; the absorption and excitation properties are addressed via TDDFT with B3LYP, PBE0, and CAM-B3LYP functionals. Based upon the calculated results, we found the following: the lower total energy of [6,6]PC_{71}BM suggests that [6,6]PC_{71}BM is more stable than [5,6]PC_{71}BM. The geometrical characters reveal that the C–C bond at the edge of six-C rings is changed from double bond in pure C_{70} fullerene to single bond in [6,6]PC_{71}BM, while the C–C bond at the edge between five-C and six-C rings is broken in [5,6]PC_{71}BM. The wave numbers of strongest IR peaks of [6,6]PC_{71}BM and [5,6]PC_{71}BM are 1219 and 1222 cm^{-1}, respectively. The Raman peaks of [6,6]PC_{71}BM and [5,6]PC_{71}BM locate at about 1609 and 1608 cm^{-1}, respectively. The vibrational modes of [6,6]PC_{71}BM and [5,6]PC_{71}BM at IR and Raman peaks are quite similar and also very similar to that of PC_{61}BM. Compared with the experimental absorption properties, it can be found that the CAM-B3LYP functional is the most suitable functional for describing excitations of PC_{71}BM. The analysis of transition configurations and MOs demonstrated that the transitions at the absorption maxima in UV/Vis region are localized π-π^* transitions in fullerenes cages. The calculated EBE for [6,6]PC_{71}BM and [5,6]PC_{71}BM are 2.08 and 2.11 eV, respectively. The smaller EBE of [6,6]PC_{71}BM is favorable for exciton dissociation in heterojunction. Furthermore, the larger isotropic polarizability of PC_{71}BM indicates that the response of PC_{71}BM to applied external electric field is stronger than that of PC_{61}BM, and therefore resulting into better nonlinear optical properties.

Acknowledgments

This work was supported by the Basic Scientific Research Foundation for Gansu Universities of China (Grant no. 1210ZTC055) and National Natural Science Foundation of China (Grant nos. 11164016 and 11164015).

References

[1] Y. Lin, Y. Li, and X. Zhan, "Small molecule semiconductors for high-efficiency organic photovoltaics," *Chemical Society Reviews*, vol. 41, no. 11, pp. 4245–4272, 2012.

[2] M. Linares, D. Beljonne, J. Cornil et al., "On the interface dipole at the pentacene-fullerene heterojunction: a theoretical study," *Journal of Physical Chemistry C*, vol. 114, no. 7, pp. 3215–3224, 2010.

[3] Y. Yi, V. Coropceanu, and J.-L. Brédas, "Exciton-dissociation and charge-recombination processes in pentacene/C_{60} solar cells: theoretical insight into the impact of interface geometry," *Journal of the American Chemical Society*, vol. 131, no. 43, pp. 15777–15783, 2009.

[4] P. W. M. Blom, V. D. Mihailetchi, L. J. A. Koster, and D. E. Markov, "Device physics of polymer:Fullerene bulk heterojunction solar cells," *Advanced Materials*, vol. 19, no. 12, pp. 1551–1566, 2007.

[5] L.-M. Chen, Z. Xu, Z. Hong, and Y. Yang, "Interface investigation and engineering—achieving high performance polymer photovoltaic devices," *Journal of Materials Chemistry*, vol. 20, no. 13, pp. 2575–2598, 2010.

[6] G. Yu, J. Gao, J. C. Hummelen, F. Wudl, and A. J. Heeger, "Polymer photovoltaic cells: enhanced efficiencies via a network of internal donor-acceptor heterojunctions," *Science*, vol. 270, no. 5243, pp. 1789–1791, 1995.

[7] F. Padinger, R. S. Rittberger, and N. S. Sariciftci, "Effects of postproduction treatment on plastic solar cells," *Advanced Functional Materials*, vol. 13, no. 1, pp. 85–88, 2003.

[8] J. Xue, B. P. Rand, S. Uchida, and S. R. Forrest, "A hybrid planar-mixed molecular heterojunction photovoltaic cell," *Advanced Materials*, vol. 17, no. 1, pp. 66–71, 2005.

[9] G. Li, V. Shrotriya, J. Huang et al., "High-efficiency solution processable polymer photovoltaic cells by self-organization of polymer blends," *Nature Materials*, vol. 4, no. 11, pp. 864–868, 2005.

[10] G. Dennler, M. C. Scharber, and C. J. Brabec, "Polymer-fullerene bulk-heterojunction solar cells," *Advanced Materials*, vol. 21, no. 13, pp. 1323–1338, 2009.

[11] N. Banerji, M. Wang, J. Fan, E. S. Chesnut, F. Wudl, and J. E. Moser, "Sensitization of fullerenes by covalent attachment of a diketopyrrolopyrrole chromophore," *Journal of Materials Chemistry*, vol. 22, no. 26, pp. 13286–13294, 2012.

[12] P. Aloukos, K. Iliopoulos, S. Couris et al., "Photophysics and transient nonlinear optical response of donor-[60]fullerene hybrids," *Journal of Materials Chemistry*, vol. 21, no. 8, pp. 2524–2534, 2011.

[13] H. Cha, D. S. Chung, S. Y. Bae et al., "Complementary absorbing star-shaped small molecules for the preparation of ternary cascade energy structures in organic photovoltaic cells," *Advanced Functional Materials*, vol. 23, no. 12, pp. 1556–1565, 2013.

[14] M. Svensson, F. Zhang, S. C. Veenstra et al., "High-performance polymer solar cells of an alternating polyfluorene copolymer and a fullerene derivative," *Advanced Materials*, vol. 15, no. 12, pp. 988–991, 2003.

[15] O. Inganäs, M. Svensson, F. Zhang et al., "Low bandgap alternating polyfluorene copolymers in plastic photodiodes and solar cells," *Applied Physics A*, vol. 79, no. 1, pp. 31–35, 2004.

[16] C. J. Brabec, A. Cravino, D. Meissner et al., "Origin of the open circuit voltage of plastic solar cells," *Advanced Functional Materials*, vol. 11, no. 5, pp. 374–380, 2001.

[17] M. M. Wienk, J. M. Kroon, W. J. H. Verhees et al., "Efficient methano[70]fullerene/MDMO-PPV bulk heterojunction photovoltaic cells," *Angewandte Chemie*, vol. 42, no. 29, pp. 3371–3375, 2003.

[18] Z. Liu, F. Xue, Y. Su, and K. Varahramyan, "Electrically bistable memory device based on spin-coated molecular complex thin film," *IEEE Electron Device Letters*, vol. 27, no. 3, pp. 151–153, 2006.

[19] Y. M. Chang and C. Y. Leu, "Conjugated polyelectrolyte and zinc oxide stacked structure as an interlayer in highly efficient and stable organic photovoltaic cells," *Journal of Materials Chemistry A*, vol. 1, no. 21, pp. 6446–6451, 2013.

[20] H.-C. Chen, I.-C. Wu, J.-H. Hung et al., "Superiority of branched side chains in spontaneous nanowire formation: exemplified by poly(3-2-methylbutylthiophene) for high-performance solar cells," *Small*, vol. 7, no. 8, pp. 1098–1107, 2011.

[21] M. Chen, W. Fu, M. Shi et al., "An ester-functionalized diketopyrrolopyrrole molecule with appropriate energy levels for application in solution-processed organic solar cells," *Journal of Materials Chemistry A*, vol. 1, no. 1, pp. 105–111, 2013.

[22] Y.-C. Chen, C.-Y. Yu, Y.-L. Fan, L.-I. Hung, C.-P. Chen, and C. Ting, "Low-bandgap conjugated polymer for high efficient photovoltaic applications," *Chemical Communications*, vol. 46, no. 35, pp. 6503–6505, 2010.

[23] P. Dutta, W. Yang, S. H. Eom, and S.-H. Lee, "Synthesis and characterization of triphenylamine flanked thiazole-based small molecules for high performance solution processed organic solar cells," *Organic Electronics*, vol. 13, no. 2, pp. 273–282, 2012.

[24] J. Jo, A. Pron, P. Berrouard et al., "A new terthiophene-thienopyrrolodione copolymer-based bulk heterojunction solar cell with high open-circuit voltage," *Advanced Energy Materials*, vol. 2, no. 11, pp. 1397–1403, 2012.

[25] D. C. Lim, K. D. Kim, S. Y. Park et al., "Towards fabrication of high-performing organic photovoltaics: new donor-polymer, atomic layer deposited thin buffer layer and plasmonic effects," *Energy & Environmental Science*, vol. 5, no. 12, pp. 9803–9807, 2012.

[26] Y. Jiang, D. Yu, L. Lu et al., "Tuning optical and electronic properties of star-shaped conjugated molecules with enlarged [small pi]-delocalization for organic solar cell application," *Journal of Materials Chemistry A*, vol. 1, no. 28, pp. 8270–8279, 2013.

[27] Y. Chen, M. Elshobaki, Z. Ye et al., "Microlens array induced light absorption enhancement in polymer solar cells," *Physical Chemistry Chemical Physics*, vol. 15, no. 12, pp. 4297–4302, 2013.

[28] R. Bauernschmitt and R. Ahlrichs, "Treatment of electronic excitations within the adiabatic approximation of time dependent density functional theory," *Chemical Physics Letters*, vol. 256, no. 4-5, pp. 454–464, 1996.

[29] C. Van Caillie and R. D. Amos, "Geometric derivatives of excitation energies using SCF and DFT," *Chemical Physics Letters*, vol. 308, no. 3-4, pp. 249–255, 1999.

[30] C. Van Caillie and R. D. Amos, "Geometric derivatives of density functional theory excitation energies using gradient-corrected functionals," *Chemical Physics Letters*, vol. 317, no. 1-2, pp. 159–164, 2000.

[31] F. Furche and R. Ahlrichs, "Adiabatic time-dependent density functional methods for excited state properties," *The Journal of Chemical Physics*, vol. 117, no. 16, pp. 7433–7447, 2002.

[32] G. Scalmani, M. J. Frisch, B. Mennucci, J. Tomasi, R. Cammi, and V. Barone, "Geometries and properties of excited states in the gas phase and in solution: theory and application of a time-dependent density functional theory polarizable continuum model," *The Journal of Chemical Physics*, vol. 124, no. 9, Article ID 094107, 2006.

[33] M. E. Casida, C. Jamorski, K. C. Casida, and D. R. Salahub, "Molecular excitation energies to high-lying bound states from time-dependent density-functional response theory: characterization and correction of the time-dependent local density approximation ionization threshold," *The Journal of Chemical Physics*, vol. 108, no. 11, pp. 4439–4449, 1998.

[34] R. E. Stratmann, G. E. Scuseria, and M. J. Frisch, "An efficient implementation of time-dependent density-functional theory for the calculation of excitation energies of large molecules," *The Journal of Chemical Physics*, vol. 109, no. 19, pp. 8218–8224, 1998.

[35] R. D. Adamson, J. P. Dombroski, and P. M. W. Gill, "Efficient calculation of short-range Coulomb energies," *Journal of Computational Chemistry*, vol. 20, no. 9, pp. 921–927, 1999.

[36] A. D. Becke, "Density-functional exchange-energy approximation with correct asymptotic behavior," *Physical Review A*, vol. 38, no. 6, pp. 3098–3100, 1988.

[37] A. D. Becke, "Density-functional thermochemistry. III. The role of exact exchange," *The Journal of Chemical Physics*, vol. 98, no. 7, pp. 5648–5652, 1993.

[38] C. Lee, W. Yang, and R. G. Parr, "Development of the Colle-Salvetti correlation-energy formula into a functional of the electron density," *Physical Review B*, vol. 37, no. 2, pp. 785–789, 1988.

[39] M. Pastore, E. Mosconi, F. De Angelis, and M. Grätzel, "A computational investigation of organic dyes for dye-sensitized solar cells: benchmark, strategies, and open issues," *Journal of Physical Chemistry C*, vol. 114, no. 15, pp. 7205–7212, 2010.

[40] J. P. Perdew, K. Burke, and M. Ernzerhof, "Generalized gradient approximation made simple," *Physical Review Letters*, vol. 78, no. 7, pp. 1396–1396, 1997.

[41] J. P. Perdew, K. Burke, and M. Ernzerhof, "Generalized gradient approximation made simple," *Physical Review Letters*, vol. 77, no. 18, pp. 3865–3868, 1996.

[42] C. Adamo and V. Barone, "Toward reliable density functional methods without adjustable parameters: the PBE0 model," *The Journal of Chemical Physics*, vol. 110, no. 13, pp. 6158–6170, 1999.

[43] T. Yanai, D. P. Tew, and N. C. Handy, "A new hybrid exchange-correlation functional using the Coulomb-attenuating method (CAM-B3LYP)," *Chemical Physics Letters*, vol. 393, no. 1–3, pp. 51–57, 2004.

[44] M. Cossi and V. Barone, "Separation between fast and slow polarizations in continuum solvation models," *Journal of Physical Chemistry A*, vol. 104, no. 46, pp. 10614–10622, 2000.

[45] D. Jacquemin, E. A. Perpete, I. Ciofini, and C. Adamo, "Accurate simulation of optical properties in dyes," *Accounts of Chemical Research*, vol. 42, no. 2, pp. 326–334, 2009.

[46] M. J. Frisch, G. W. Trucks, H. B. Schlegel et al., Gaussian, Inc., Wallingford, Conn, USA, 2010.

[47] W. H. Powell, F. Cozzi, G. P. Moss, C. Thilgen, R. J.-R. Hwu, and A. Yerin, "Nomenclature for the C_{60}-I_h and C_{70}-$D_{5h(6)}$ fullerenes: (IUPAC recommendations 2002)," *Pure and Applied Chemistry*, vol. 74, no. 4, pp. 629–695, 2002.

[48] T.-T. Wang and H.-P. Zeng, "Synthesis, characterization and theoretical calculation of the fulleropyrrolidines containing triphenylamine," *Chinese Journal of Chemistry*, vol. 24, no. 2, pp. 224–230, 2006.

[49] C. Zhang, W. Liang, H. Chen, Y. Chen, Z. Wei, and Y. Wu, "Theoretical studies on the geometrical and electronic structures of N-methyle-3,4-fulleropyrrolidine," *Journal of Molecular Structure: THEOCHEM*, vol. 862, no. 1–3, pp. 98–104, 2008.

[50] C.-R. Zhang, H.-S. Chen, Y.-H. Chen, Z.-Q. Wei, and Z.-S. Pu, "DFT study on methanofullerene derivative [6,6]-Phenyl-C_{61} butyric acid methyl ester," *Acta Physico-Chimica Sinica*, vol. 24, no. 8, pp. 1353–1358, 2008.

[51] B.-G. Kim, C.-G. Zhen, E. J. Jeong, J. Kieffer, and J. Kim, "Organic dye design tools for efficient photocurrent generation in dye-sensitized solar cells: exciton binding energy and electron acceptors," *Advanced Functional Materials*, vol. 22, no. 8, pp. 1606–1612, 2012.

[52] B. A. Gregg, "Excitonic solar cells," *Journal of Physical Chemistry B*, vol. 107, no. 20, pp. 4688–4698, 2003.

[53] G. D. Scholes and G. Rumbles, "Excitons in nanoscale systems," *Nature Materials*, vol. 5, no. 9, pp. 683–696, 2006.

[54] C.-R. Zhang, H.-S. Chen, and G.-H. Wang, "Structure and properties of semiconductor microclusters Ga_nP_n(n=*l*–*4*): a first principle study," *Chemical Research in Chinese Universities*, vol. 20, no. 5, pp. 640–646, 2004.

[55] H. Cheng, J. K. Feng, A. M. Ren, and L. Jian-Jun, "Theoretical study of the structure, spectra and nonlinear third-order optical susceptibility of C_{74}," *Acta Chimica Sinica*, vol. 60, no. 5, pp. 830–834, 2002.

[56] H. Cheng, J.-K. Feng, A.-M. Ren, and J.-J. Liu, "Theoretical study of the structure, spectra and nonlinear optical susceptibility of C_{72}," *Acta Chimica Sinica*, vol. 61, no. 4, pp. 541–546, 2003.